

Rational Methods of Plastic Deformation Providing Formation of Ultrafine-Grained Structure in Large-Sized Products

F.Z. Utyashev , A.V. Botkin , E.P. Volkova* , R.Z. Valiev 

Ufa University of Science and Technology, Ufa, 450076, Russia

Article history

Received March 14, 2024
Accepted March 20, 2024
Available online March 31, 2024

Abstract

Based on the peculiarities of plastic deformation mechanics and physical mesomechanics, the processes are considered and technological schemes for their realization are proposed to ensure the formation of ultrafine-grained structure in axisymmetric products of large sizes. Deformation of coarse-grained materials in temperature-velocity conditions of superplastic deformation and methods of severe plastic deformation are taken as methods of preparation of such a structure. All of these deformations include large strain, and they are carried out at low hydraulic press speeds, but at different temperatures: in the mode of superplasticity at hot temperatures, and in the mode of severe plastic deformation at warm or cold temperature deformation. The first mode allows grains to be refined to microcrystalline sizes of 1–10 microns, and such a material acquires the ability to deform in a state of superplasticity, i.e., in tension with low resistance to deformation and high elongation. The second mode (severe plastic deformation) refines grains to submicro- ($1 \div 0.1 \mu\text{m}$) and nanosizes (less than $0.1 \mu\text{m}$), thus giving metal materials record structural strength, as well as the possibility to use processing in extended temperature-velocity conditions of superplastic deformation in comparison with microcrystalline structure.

Keywords: Ultrafine-grained structure; Superplastic deformation; Severe plastic deformation; Shear and rotational deformations; Torsion with upset or tension

1. INTRODUCTION

The continuing interest of engineering and technical specialists in ultrafine-grained (UFG) materials is due to their high physical, mechanical and technological properties, which allow to ensure the scientific and technological development of aircraft engine building, as well as health care [1,2]. In the recent past, UFG materials included metals and alloys with grain sizes of no more than 10 microns, demonstrating high superplastic properties under certain temperature-velocity conditions [3,4]. Later, in order to expand the temperature-velocity conditions of superplastic deformation, interest arose in obtaining materials with smaller equiaxed grains with sizes less than 1 micron. To obtain such materials, severe plastic deformation (SPD) methods were proposed and developed [5,6]. As a result, materials with submicro- and nanometric grains were obtained, which made it possible to reduce the temperature

and increase the rate of superplastic deformation. Moreover, a number of physical properties of such materials, which were previously considered independent of grain size, have significantly changed. For this reason, UFG materials usually include materials with a grain size of less than 1 micron.

This work considers the production and properties of alloys with an average grain size from 10 microns and up to several nanosizes, i.e. to sizes less than 0.1 micron, since their development is associated with very labor-intensive methods for accumulating final, i.e., large and extremely large uniform deformations, especially in workpieces with significant dimensions, $\geq 100 \text{ mm}$. It should be noted that in continuum mechanics [7] finite deformations of solids include deformations with a degree of ≥ 1 , leading to a radical change in their properties. Since in this discipline the structure of metallic materials is assumed to be continuous, we usually mean only the shape-

* Corresponding author: E.P. Volkova, e-mail: epvolkova@mail.ru

changing (shear) component of deformation taken into account in the calculations. In the physics of strength and plasticity [8,9], along with the shear component, the crystal structure of metallic materials is also influenced by the rotational component, which is especially important in the technological processes of manufacturing large-sized UFG semi-finished products. For this reason, such processes can be classified as methods that provide extremely large deformations.

Traditionally, as already noted, SPD methods are carried out under conditions of warm (semi-hot) or cold deformation. Under these conditions, starting from degrees of deformation above 0.2–0.3 after the formation of a cellular structure, mesodefects appear in metals and alloys—collective forms of dislocations known as partial disclinations [10,11]. The movements of these defects along dense accumulations of dislocations, which are imperfect low-angle cell boundaries that permanently appear during deformation, lead to the formation of various mesobands. Including the thinnest of them—deformation microbands. Multiple intersections of microbands, as well as shear microbands replacing them [12], due to the non-monotonic nature of deformation during SPD, lead to the formation of a network of grain boundaries of submicro- (less than 1 μm) and nanometric ($\sim 0.1 \mu\text{m}$) sizes.

It is advisable to obtain a microcrystalline UFG structure with an average grain size ($1\div 10 \mu\text{m}$) by deforming coarse-grained materials under temperature and speed conditions characteristic of superplasticity [13]. This process is known as deformation in the superplastic deformation regime [14]. For massive workpieces made of heterophase, low-plasticity and difficult-to-deform materials, it is usually carried out by means of all-round volumetric forging or by multi-transition fractional upsetting [1]. The formation of UFG structure in heat-resistant alloys based on nickel and titanium used in the fabrication of disks for gas turbine engines (GTE) under superplastic deformation conditions is of great interest. However, forging and fractional upsetting processes are extremely labor intensive and have low metal utilization rates (MURs) due to cracking. An exception for these alloys is the “gatorising” pressing process used in a number of Western companies, which makes it possible to obtain rods with a diameter of 300 mm with a uniform microcrystalline structure and gas turbine engine disks with a diameter of over 500 millimeters or more [15,16]. The implementation of such a process in Russia is hampered by the lack of powerful (over 18,000 tons) horizontal hydraulic presses and expensive vacuum-stamping complexes [17].

The purpose of this work is to determine the conditions of deformation and propose process flow diagrams for the

production of UFG semi-finished products in the form of disks and rods of large diameters, for a minimum number of operations and high material utilization factor, using deformation in the SPD and superplasticity modes. To describe the features of structure formation during SPD, the article discusses commonly used methods: high pressure torsion (HPT) and equal-channel angular pressing (ECAP). Currently, they are used mainly in laboratories to obtain UFG structures in small disks and rods with a diameter of $\sim 10\div 25 \text{ mm}$. In the case of deformation in the superplasticity regime, we use data on structure formation occurring during the rolling out of gas turbine engine disks of large diameters 600–800 mm from coarse-grained billets of heat-resistant alloys [13]. Due to the lack of equipment in industrial workshops with mills for rolling out disks and rods, this process is used only in experimental productions. As an alternative to the “gatorising” process, we will substantiate the production of UFG structure in large-sized disks and rods using the processes of upsetting with torsion and stretching with torsion, both in the superplastic deformation regime and SPD.

2. FEATURES OF THE MECHANICS OF LARGE STRAINS AND MESOMECHANICS OF STRUCTURAL FORMATION

2.1. Mechanical features

To analyze large plastic deformations, it is necessary to use finite strain tensors [18]. However, analysis of the deformed state using such tensors significantly complicates the solution of the problem due to the need to take into account not only the first partial derivatives of the displacement components, but also their products. Therefore, we will limit ourselves to the definition of a scalar quantity: the accumulated true (logarithmic) deformation with certain vector properties that evaluate the history of deformation. Let us consider the indicated approach using the example of torsion under pressure¹. Such deformation can be realized in two versions: as torsion with settlement and as torsion with tension². The difference between them is the direction of the pressure generated by the axial force. In the case of upsetting, it leads to the production of a gas turbine engine disk if an isothermal stamp is used [19] and pressure is created, upsetting the workpiece with simultaneous plastic torsion. In the case of tension with torsion, such deformation leads to the production of a cylindrical rod based on a device that implements, for example, the method [20]. In this method, torsion and axial pressure of variable sign (first tensile and then compressive) are carried out in the

¹ In metal forming, this method is known as torsional upsetting.

² From the standpoint of deformation mechanics, these processes are largely described by identical equations.

local zone of the rod—an artificially created neck—which, as the grains are refined, is sequentially moved along the length of the rod [13,20].

Returning to the deformation tensor, we note that if we differentiate it with respect to time, excluding high-order derivatives, we obtain the deformation rate tensor ξ_{ij} :

$$\{\xi_{ij}\} = \begin{pmatrix} -v/2L & 0 & 0 \\ 0 & -v/2L & r\omega/2L \\ 0 & r\omega/2L & v/L \end{pmatrix}, \quad (1)$$

where $v = dL/dt$ is the linear speed of movement of the active tool, $\omega = d\varphi/dt$ is the angular speed of rotation (φ is the angular polar coordinate, t is time), L and r are current length and radius of the sample, respectively.

The intensity of the strain rate ξ_e is determined as the square root of the absolute value of the second invariant of this tensor:

$$\xi_e = \sqrt{\frac{2}{3}\xi_{ij}\xi_{ij}} = \frac{1}{L}\sqrt{v^2 + \frac{r^2\omega^2}{3}}. \quad (2)$$

We calculate the accumulated true deformation ε (degree of deformation) using the Smirnov-Alyaeu equation [21], integrating the deformation rate along the deformation trajectory:

$$\varepsilon = \int \xi_e dt = \int (\xi_{ij}\xi_{ij})^{1/2} dt. \quad (3)$$

Solving this equation under pressure torsion leads to a cumbersome equation that includes contributions from shear and rotational components:

$$\varepsilon = 2\sqrt{1 + \frac{\theta^2}{3}} - 2\sqrt{1 + \frac{\theta^2}{3(1 + \varepsilon_a)}} + \ln(1 + \varepsilon_a) + \ln \frac{1 + \frac{\theta^2}{6(1 + \varepsilon_a)} + \sqrt{1 + \frac{\theta^2}{3(1 + \varepsilon_a)}}}{1 + \frac{\theta^2}{6} + \sqrt{1 + \frac{\theta^2}{3}}}, \quad (4)$$

where $\varepsilon_a = vt/L_0$ and $\theta = r_0\omega/v$; L_0 and r_0 are initial values of the radius and length of the sample, respectively. Parameter ε_a is the axial deformation due to the action of an axial force. Parameter θ represents the ratio of the circumferential velocity to the linear axial velocity for the external points of the sample at the initial moment of deformation, i.e., relative magnitude of the rotational component of deformation.

It is convenient to evaluate the contributions of the shear and rotational components to the accumulated deformation and their relationships during torsion under the pressure of the disk using the concept of the deformation trajectory. Since in a closed die the disk thins slightly and

does not change in diameter, we introduce a two-dimensional coordinate system: with component e_1 , showing the degree of axial deformation (thinning) and with component e_2 , showing the degree of rotational deformation (twisting). We obtain

$$(de)^2 = (de_1)^2 + (de_2)^2, \quad (5)$$

where $de_1 = dL/L$, $de_2 = rd\varphi/(L\sqrt{3})$.

Next, we introduce the vector

$$\mathbf{e} = e_1\mathbf{i} + e_2\mathbf{j}, \quad (6)$$

where $e_1 = \ln(L/L_0)$, $e_2 = \int (r/(L\sqrt{3}))d\varphi$.

The total deformation ε is determined by the length of the vector $(e_1^2 + e_2^2)^{1/2}$. Fig. 1 shows three variants of the deformation trajectory obtained at different ratios $k = e_1/e_2$.

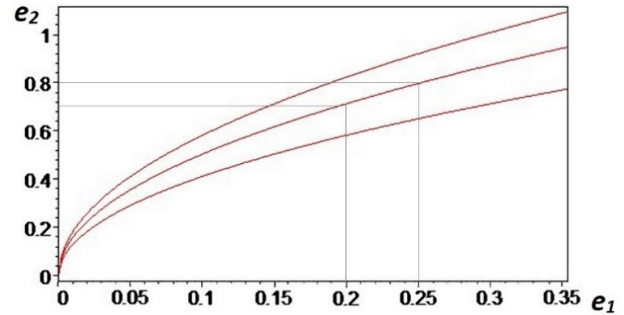


Fig. 1. Deformation trajectories at values $k = 1$ (lower curve), $k = 2$ (middle curve) and $k = 3$ (upper curve).

It can be seen that an increase in k leads to a significant increase in the rotational component in comparison with the shear component. Setting the ratio k between the contributions of the rotational and shear components of the deformations makes it possible to determine the conditions that provide, during upsetting with torsion, a technologically advantageous amount of deformation for the formation of UFG structure in disks of large diameters. Note that in an isothermal die, in order to ensure a uniform temperature field in the deformation zone, it is advisable to reduce the proportion of the shear component (i.e., reduce the height of the workpiece and, accordingly, the height of the working area of the die, which is difficult to insulate from heat loss) and increase the proportion of the rotational component.

2.2. Mechanics and mesomechanics of rolling

A detailed description of the rolling process, if necessary, can be found in monographs [1,13]. Here, as a general idea of the process, Fig. 2 shows a diagram of the workpiece rolling and the macro- and microstructure of the rolled disk.

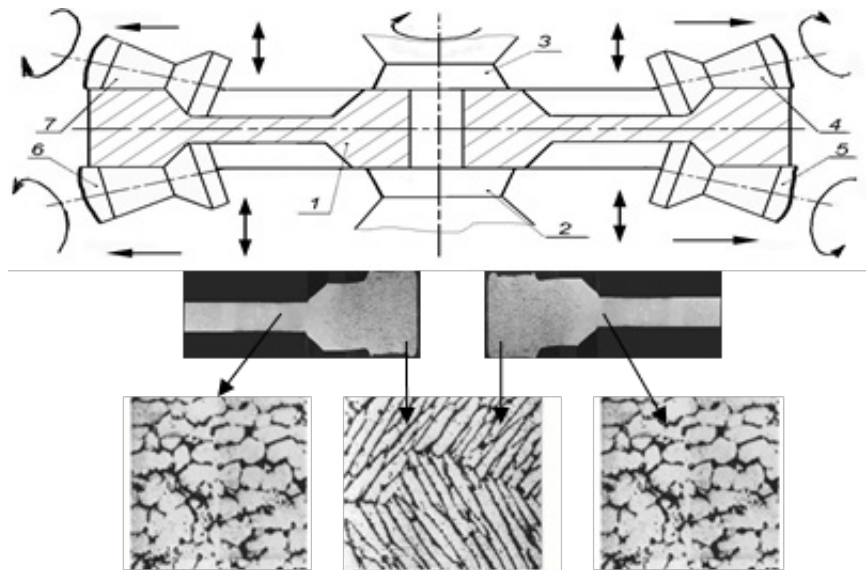


Fig. 2. Scheme of rolling out the workpiece and the macro- and microstructure of the rolled disk.

At the top of the diagram (Fig. 2) there is a titanium disk blank, rolled out by two pairs of rollers (4–7), compressing the rim of the blank and moving along its radius. At the bottom of the diagram, macro- and microstructures are shown in the disk hub, where the original lamellar coarse-grained structure was preserved, and in the disk web, where a globular UFG structure was formed. The structure in the rim is not shown, it, like in the hub, is worked out insignificantly.

According to the scheme, a workpiece with a coarse-grained lamellar structure is rotated by quills and deformed by one or, to increase productivity, two pairs of rollers moving along the radius. At the same time, at each revolution, the rollers compress the rim of the workpiece reducing its thickness and, thereby, forming the disk blade.

For definiteness, we indicate a twofold decrease in the thickness of the rim, for example from 60 to 30 mm, and an increase in the radius of the disk from 200 to 400 mm. The trajectory of movement of the rollers relative to the workpiece, along which the center of the deformation center shifts, is an Archimedes spiral $L = R\varphi$.

To analyze the accumulated deformation in the disk surface, we use the concept of J. Lagrange in relation to the study of the movement of material points (MPs) of a continuous medium [7]. The essence of this concept is that MPs during plastic deformation necessarily move along physical trajectories specified by the tool, which, in fact, leads to a change in the shape of the solid body. The role of MPs in a crystalline body, according to J. Friedel [22], is played by edge dislocations. Let us set the position of the MP by the radius vector \mathbf{R} . Then the speed of the MP moving along the physical trajectory of mass transfer can be expressed by the equation:

$$\mathbf{V} = \frac{d\mathbf{R}}{dt} = \frac{d\mathbf{R}}{dL} \frac{dL}{dt} = \boldsymbol{\tau} \frac{dL}{dt} = \boldsymbol{\tau}V, \tag{7}$$

where $\boldsymbol{\tau}$ is unit vector directed tangentially to the trajectory of the particle, L is trajectory length and \mathbf{V} is velocity vector.

From this we obtain that the degree of deformation is determined by the sum of integrals that take into account the contribution of the shear component, i.e. radial displacement and rotational components.

$$\begin{aligned} \varepsilon &= \int_0^t \frac{V}{L} dt = \int \frac{dL}{L} = \int \frac{\varphi dR + R d\varphi}{R\varphi} \\ &= \int \frac{dR}{R} + \int \frac{d\varphi}{\varphi}. \end{aligned} \tag{8}$$

To solve equation (8), it is convenient to use the Archimedes spiral equation in polar coordinates:

$$\frac{R}{a} = \frac{\varphi}{2\pi}, \tag{9}$$

where a is the spiral pitch equal to the radial displacement of the rollers per revolution.

Then $R = a\varphi / (2\pi)$, $L = R\varphi = a\varphi^2 / (2\pi)$. From this we obtain that each of the contributions in equation (8) is equal to 0.69, and the total degree of logarithmic deformation will be ≈ 1.4 .

Systematic studies of structural changes observed in many coarse-grained alloys during their deformation under temperature-speed conditions of superplasticity, i.e., usually at a homologous temperature above $0.5T_m$ and strain rates of $10^{-3} \div 10^{-2} \text{ s}^{-1}$, lead to the development of dynamic recrystallization [1,13]. In areas where, as a result of upsetting or stamping, a relative deformation of

over 60÷70% a microcrystalline structure is formed. To form such a structure throughout the entire volume of a large-sized workpiece, comprehensive forging is used. For example, such forging was carried out for a workpiece made of titanium alloy VT6 [23] with a consistent decrease in temperature from 950 °C to 500 °C and with limited relative deformation ($\approx 50\%$) in the transitions. As a result, we obtained a homogeneous UFG structure with a grain size of $\sim 0.5 \mu\text{m}$ in a massive rod with a diameter of $\sim 150 \text{ mm}$ and a length of 200 mm. This publication does not indicate the amount of deformation spent on grain refinement, however, it is not difficult to estimate. Even with a relatively limited number of transitions $\sim 10\div 20$, depending on the weight of the workpiece, a significant amount of shear strain is required—over 7÷14 units. Such large deformations, the difficulty of automating all-round forging and, accordingly, the extremely high labor intensity of manual labor limit the use of this process in industry.

For all SPD methods, as in forging, the non-monotonicity of the deformation process is important. From the standpoint of mesomechanics, structure formation in this case is quite logically explained by the permanent evolution of the formation and movement of linear defects—partial disclinations. In monotonic processes, these defects form the boundaries of stripes directed towards the drawing of the workpiece, and in non-monotonic processes, the direction of the stripes changes in accordance with the change in the orientation of the strain tensor. During monotonic fractional rolling of nickel, it was shown [24] that the boundaries of stripes of different thicknesses are formed as low-angle boundaries in the direction of elongation of the workpiece, and are called geometrically necessary boundaries. Within the stripes, low-angle cell boundaries, called random, are observed. As the true strain accumulated to 4.5, the thickness of the stripes decreased to $1\div 2 \mu\text{m}$, while only a small part of the microstripes acquired high-angle misorientations, and the random cell boundaries remained the same low-angle. In works [10,25], where other monotonic deformation processes were used, in particular, drawing, the boundaries of stripes in various metals formed by the movements of partial disclinations are called boundaries of deformation origin. These boundaries, like the boundaries of the stripes after rolling, acquired a morphology close to rectilinear and are directed along the drawing of the material. In addition, during deformation, microstripes fragment into sections whose length is an order of magnitude greater than their thickness, which, according to [26], is due to the effect of transverse disturbances on various laminar formations that arise in metals.

In modern studies devoted to structure formation in metals and alloys during SPD by torsion under pressure [27,28], stripe structures are called fragmentation stripes. In contrast to elongated fragments with low-angle boundaries that arise during monotonic deformation, non-monotonic torsion under pressure leads to the formation of equiaxed grains (sub-microcrystallites) $0.1\div 1 \mu\text{m}$ in size with high-angle boundaries. The authors characterized the mechanism of structure refinement as dislocation-disclination reorientation of the crystal lattice.

Thus, from the above-mentioned publications it follows that the refinement of the structure under large and ultra-large plastic deformation is largely due to the evolution of mesodefects, which depends on the kinematics of the material flow in the deformation zone.

3. ROLE OF FLOW KINEMATICS IN STRUCTURE FORMATION

During monotonic deformations, in particular during longitudinal rolling, the flow of the metal is determined by the total effect of the rolls on the angular velocity of rotation of MPs³ in the deformation zone. With a certain change in the radius of rotation between atoms located in adjacent planes of the crystal lattice, a jump in the angular velocity $\Delta\omega$ occurs, leading to misorientation of the planes by an angle $\varphi = \Delta\omega t$, where t is the time the MPs (atoms) are in the deformation zone. As a result, the distance between atoms becomes greater than the lattice parameter, which, in fact, leads to the formation of a stripe boundary. The flow of metal is divided into a family of stripes, the thickness and peripheral speed of which increase towards the longitudinal axis of the workpiece, at which the difference in the moments and speeds of the impact of the rolls on the workpiece is leveled to zero. Since large deformation in a thin-walled workpiece accumulates as a result of many passes with small degrees of deformation, and also due to the fact that the angular velocity of the workpiece in the deformation zone is determined by the difference in the speeds of the rollers bending the workpiece in opposite directions, then during rolling as a whole weakly curved laminar stripes are formed, separated in the longitudinal direction, as already noted, along the length into parts—fragments.

Compared to monotonic deformation, the kinematics of material flow during non-monotonic deformation of the material in SPD methods is more complex [29,30]. It is convenient to first consider it using the example of ECAP of a rod with a square cross-section, then highlight the features of the flow of material in a thin disk during HPT.

³ By definition in continuum mechanics MP is an infinitesimal quantity. In a crystalline material, we take the atom as a material point.

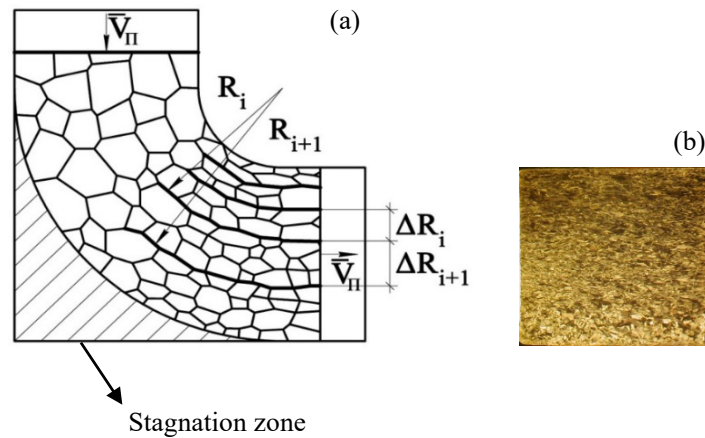


Fig. 3. Formation of curved microstripes with cells inside in the deformation zone during ECAP and coarsening of the macrostructure in the cross section with increasing radius of rotation R in the zone of formation of thickened stripes.

The ECAP process is usually depicted as a simple shear that occurs when a rod passes through the bisector of the angle of intersection of the channels. However, with such a simplification, an unrealistically singular increase in the rate of deformation ξ of the material will appear on the bisector line: $\Delta V / L = \xi \rightarrow \infty$, since the thickness of the bisector $L = 0$. A plausible change in the transfer speed of the workpiece along the channel does not occur abruptly on the bisector, but gradually along the arcs of material movement in a sufficiently large sector. The formation of such a sector is due to the appearance of a stagnation zone—a part torn off from the workpiece, stuck in the widened angle of intersection of the channels. In a device with orthogonal intersection of channels, this sector has a shape in longitudinal section close to one-fourth of a circle. The narrow part of the sector is limited by a small arc with a small radius of crushing the sharp apex of the angle of intersection of the channels, and the widened part of the sector is limited by a large arc outlined by a radius equal to the distance between the walls of the channels. As a result, of a sequential rotation of the flow velocity of MPs, directed tangentially to the arcs, a family of stripes appears in the source, the thickness of which increases with increasing arc radius, Fig. 3. The rotation speed of MPs (“atoms”) in each stripe, as well as during rolling, is constant in magnitude and equal to the speed of the punch.

At the same time, bending of the stripes in the deformation zone leads to mass transfer of material from the compression zone to the tension zone, i.e. from the border of a stripe of smaller radius to the border of a stripe of large radius. Such mass transfer during bending of a metal stripe, as noted earlier [22], leads to the movement of edge dislocations in the direction of minimal trajectories, which are involutes.

The flow of MPs in the workpiece stripes along the channel axis occurs with one portable (in the deformation zone) peripheral speed equal to the speed of the punch. At

the same time, from the analysis of the kinematics of the flow rate of mass transfer of MPs along involutes, it follows that in addition to the peripheral speed in the stripes, transverse speed and the corresponding shear, shape-changing and rotational components of the workpiece deformation arise [8].

Graphs of the dependence of these components on the angle of intersection of the channels in the ECAP device are shown in Fig. 4. It can be seen that graph 1', constructed using the well-known formula $\varepsilon = (2/\sqrt{3}) \cot(\omega/2)$ [31] is close to the shear strain value. Meanwhile, the value of the rotational deformation is almost twice as large as the contribution of the shear component, and the contribution of the sum of the two components is 3 times greater.

The presence of a rotational component of deformation makes it possible to explain the increase in misorientations of low-angle stripe boundaries during ECAP and other SPD methods. Indeed, when stripe structures are born as low-angle boundaries of dislocation origin, angular misorientations increase with the accumulation of deformation.

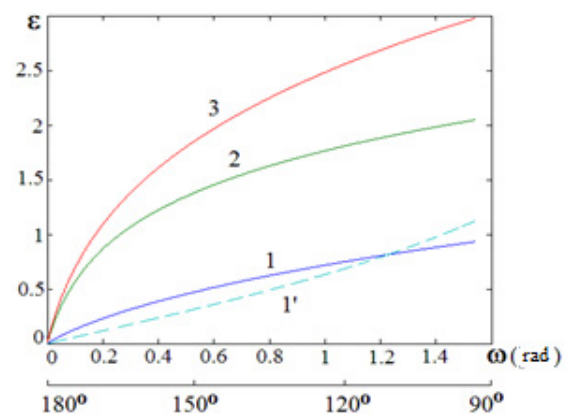


Fig. 4. Dependence of the total deformation (curve 3), its rotational (2) and shear (1) components on the angle of intersection of channels during ECAP. Curve 1', constructed according to formula [31], is shown for comparison.

In accordance with modern concepts, this occurs due to their capture (adsorption) of lattice dislocations.

From the fact of the formation of small grains with predominantly high-angle boundaries after SPD, it follows that the nature of low-angle boundaries of deformation origin, which are the product of mesodefekt movements, is fundamentally different from that of low-angle cell boundaries.

In the absence of movements along imperfect cell boundaries, they only improve without changing their low-angle misorientations [32].

The radius of bending (rotation) of stripe boundaries plays an important role in structure formation during ECAP. With its increase, the thickness of the microstripes, the number and sizes of the low-angle cells contained in them increase, which leads to the formation of a heterogeneous structure in the cross section of the rod after one pass. For this reason, ECAP uses multi-pass pressing, with the workpiece rotated 90 degrees around the longitudinal axis before each pass. This leads to multiple intersections of microstripes boundaries and the formation of a fine network of grain boundaries in almost the entire cross section of the rod. In the case of ECAP of thick rods ~ 60 mm, grain refinement in the rod is not achieved. In this regard, it is important to use the scheme given in Ref. [13], in which ECAP is combined with torsion of the rod in the deformation zone.

The deformation pattern of a thin disk during HPT in a closed die, like the ECAP of a rod, can be classified as a flat deformation pattern. The disk is first loaded with pressure, it acquires a minimum thickness, a developed contact patch with the striker is created, and then it is subjected to torsion [2]. The generatrix of the lateral surface of the disk is twisted along a stepped helical line (Fig. 5), which is divided into horizontal sections along which microstripes slide. Such microstripes are observed in chordal (transverse) sections of the disk.

Following the principle of ensuring compatibility of deformation, the velocity field in the plane normal to the axis of the disk can be taken to be the same as the velocity field in the longitudinal section of the channels during ECAP with the difference that during HPT the rotation of the

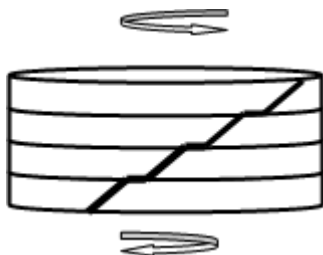


Fig. 5. Scheme of disk torsion and formation of thin ($\leq 0.1 \mu\text{m}$) microstripe layers, sliding along the boundaries which leads to a stepped helix shape.

stripes is not carried out at an angle $\leq n\pi/2$ rad, where n is the number of passes during ECAP, but continuously by $2\pi n$ radians, where n is the number of revolutions. Based on the number of revolutions, the value of the rotational component of deformation during HPT will be determined by the value $2\pi n / 0.5\pi = 4n$. Thus, with HPT, a greater number of deformation microstripes and their intersections are formed than with ECAP due to the subsequent formation of shear microstripes and a finer network of grain boundaries.

4. INFLUENCE OF ENERGY-POWER PARAMETERS OF HPT ON STRUCTURE FORMATION

The axial force P_z and moment M for the considered deformation schemes by torsion under pressure will be determined under the assumption that the workpiece material is isotropic incompressible, the process is isothermal and homogeneous in the case of upsetting, and in the case of tension, the deformation is localized in a neck artificially created by rollers, which is sequentially moved along the rod. At the end of torsion in the neck, the rod is compressed to its original dimensions in order to return to the original diameter. Full processing is completed after a series of deformations of the journals and the return of the diameter of the rod along the entire length.

The power balance of the work of internal and external forces during combined deformation has the form:

$$N_{in} = \iiint_V \tau H dV = \iiint_V \sigma_e \xi_e dV = Pv + M\omega. \quad (10)$$

Here N_{in} is the power from internal forces, σ_e is stress intensity, ξ_e is intensity of strain rate, P is axial force (upsetting or tensile force), v is strain rate during upsetting or extension, M is torque, ω is angular velocity of torsion. For given v and ω , as well as in the general case in the presence of external hydrostatic pressure p_0 , it is possible to determine P and M . If we use the hypothesis about the proportionality of the deviators of strain rates and stresses S_i , then the stress deviator has the form similar to the deviator of strain rates:

$$S_{ij} = \begin{pmatrix} S_{rr} & 0 & 0 \\ 0 & S_{\varphi\varphi} & S_{\varphi z} \\ 0 & S_{z\varphi} & S_{zz} \end{pmatrix}. \quad (11)$$

Then the same relationships exist between the stress components as between the velocity deviator components, i.e., $S_{rr} = S_{\varphi\varphi} = -S_{zz} / 2$ and, since $S_{\varphi z} / S_{zz} = \xi_{\varphi z} / \xi_{zz} = (r\omega / 2l) / (v/l) = r\omega / 2v$, then $S_{\varphi z} = (r\omega / 2v)S_{zz}$.

Hence, the stress intensity:

$$\sigma_e = \sqrt{\frac{3}{2} S_{ij} S_{ij}} = \frac{3}{2} S_{zz} \sqrt{1 + \frac{r^2 \omega^2}{3v^2}}. \quad (12)$$

The equations of motion of a continuous medium in a cylindrical coordinate system under isothermal deformation (without taking into account inertia and acceleration, as well as without changing the density of the material) are reduced to the equilibrium equations:

$$\begin{aligned} d\sigma_{rr} / dz = 0 &\Rightarrow \sigma_{rr} = \sigma_{rr}(r), \\ d\sigma_{\varphi z} / dz = 0 &\Rightarrow \sigma_{\varphi z} = \sigma_{\varphi z}(r), \\ d\sigma_{zz} / dz = 0 &\Rightarrow \sigma_{zz} = \sigma_{zz}(r). \end{aligned} \tag{13}$$

The components of the stress tensor are found using mixed boundary conditions in which the axial v and angular ω velocities of movement of the end sections of the deformable rod are specified. In addition, we accept the force condition:

$$\sigma_{rr} \Big|_{r=R} = 0. \tag{14}$$

Hence, for stretching with torsion,

$$\begin{aligned} \sigma_{zz} &= \frac{\sigma_e}{\sqrt{1 + \frac{r^2 \omega^2}{3V^2}}}, \\ \sigma_{rr} = \sigma_{\varphi\varphi} &= 0, \end{aligned} \tag{15}$$

and for compression with torsion

$$\begin{aligned} \sigma_{rr} = \sigma_{\varphi\varphi} &= 0, \\ \sigma_{zz} &= -\frac{\sigma_e}{\sqrt{1 + \frac{r^2 \omega^2}{3V^2}}}. \end{aligned} \tag{16}$$

The magnitude of the axial force for tension (compression) with torsion, without taking into account the influence of non-deformable parts of the rod, to the left and right of the neck, as well as in the case of upsetting with torsion, without taking into account contact friction forces:

$$P_z = \iint_S |\sigma_{zz}| dS = \int_0^{d/2} \frac{2\pi r \sigma_e}{\sqrt{1 + \frac{r^2 \omega^2}{3V^2}}} dr, \tag{17}$$

where the integration region S is the cross-sectional area of a rod with diameter d . The integrand in Eq. (17) is the law of tool pressure distribution on the end surface of the workpiece.

Applying the mean value theorem to (14), we obtain:

$$P_z \approx \frac{\pi \sigma_e d^2}{4 \sqrt{1 + \frac{d^2 \omega^2}{48V^2}}}. \tag{18}$$

In the case of closed upset with torsion:

$$P_z = \iint_S \left(\frac{\sigma_e}{\sqrt{1 + \frac{r^2 \omega^2}{3V^2}}} + p_0 \right) dS, \tag{19}$$

where p_0 is the positive hydrostatic pressure created by the contact pressure acting on the lateral surface of the matrix.

Substituting the deformation rate (2) and the axial force (18) into Eq. (10), we obtain the formula for the moment:

$$M \approx \frac{\pi \sigma_e \omega d^4}{48 \sqrt{16V^2 + \frac{d^2 \omega^2}{3}}}. \tag{20}$$

With low sensitivity of the intensity of metal stresses to the rate of deformation, the pressure distribution during upsetting with torsion of the disk along the contact surface, even in the absence of friction forces, is uneven. It is maximum in the center of the workpiece, and decreases towards the edge of the end surface of the disk according to a quadratic dependence on the radius. For this reason, with an increase in the diameter of the disk, to ensure uniform settlement, it is necessary to significantly increase the pressure of the strikers, so that at the periphery of the end surface the pressure becomes greater than the material resistance σ_s . Since increasing pressure reduces tool life, it is important to evaluate the factors that reduce axial force.

4.1. Possibility of reducing axial force during HPT

The magnitude of the reduction in axial force during upsetting with torsion, according to literature data [14], varies by an order of magnitude—from 2 to 20 times. Such a significant spread in the force of upsetting during torsion is due not only to the conditions of deformation and strength properties of the workpiece material, but also to the conditions of torque transfer from the tool to the workpiece. If the moment is transmitted due to friction between the workpiece and the tool, then a reduction in the force during upsetting with torsion is achieved due to the “reversal” of the vector of contact friction forces between the striker and the end of the workpiece.

In vector form, the friction force \mathbf{f} on the contact surface is equal to the sum of the radial and tangential components:

$$\mathbf{f} = \mathbf{f}_r + \mathbf{f}_t. \tag{21}$$

The radial component \mathbf{f}_r is a reactive force that prevents an increase in the end surface area of the workpiece. In the limit, it should be reduced to zero; accordingly, the friction coefficient in the radial direction should be as small as possible. The tangential component \mathbf{f}_t is an active friction force; it is necessary to transmit the torsional moment of the workpiece. Therefore, for reliable transmission of torsional torque without sliding, the friction coefficient in the circumferential direction must be maximum. Thus, if we ensure a minimum friction coefficient in the radial direction and a maximum in the circumferential direction, then during upsetting with torsion we will ensure

a reduction in the axial force and the amount of pressure on the workpiece and the strikers.

The results of experiments and calculations show that a decrease in the magnitude of the deforming force is also observed when the rod is stretched with torsion, in which plastic torsion of the rod is carried out by means of grippers. The reason for the reduction in force in this case is due to overcoming the internal friction of the workpiece. Since the rod is subjected to torsion and tension, the stress intensity required for deformation can be represented as the sum of the stresses induced by the torsional moment and axial force. The torque activates the generation of lattice dislocations by dislocation sources. Then the role of the axial force is reduced only to the creation of stresses necessary for dislocations to overcome internal friction (Peierls forces) as they slide in a direction that ensures elongation of the rod. Thus, the combination of moment and axial force helps to reduce the latter, which is especially important for reducing contact stresses on the tool surface during torsional upsetting.

5. DESIGN AND TECHNOLOGICAL VARIATIONS FOR THE MANUFACTURE OF LARGE RODS AND DISCS WITH UFG STRUCTURE USING SUPERPLASTIC DEFORMATION AND SPD

Of significant importance for practice is the implementation of SPD methods, which make it possible to obtain UFG structure and high properties in bulk products with dimensions of tens and hundreds of millimeters. These methods are combined deformations with the simultaneous use of torsion with upsetting or tension.

5.1. Production of UFG rods

A sample with a diameter of 100 mm and a length of 700 mm was made from a hot-forged heat-resistant titanium alloy VT9 with a coarse-grained plate structure (Fig. 6) and

subjected to combined deformation. The sample was installed in the furnace of an experimental rolling mill SRD800 [1,13], which allows such deformation in the neck area, was heated to 950 °C and the sample neck was twisted by 2160 degrees (6 revolutions) at a speed of 0.6 rpm with simultaneous stretching by 15 mm, $\sigma_e = \sigma_s = 100$ MPa.

The calculated values of the axial force and moment according to formulas (18), (20) are 21.7 kN and 3.13 N·m, respectively. Metallographic studies showed that a globular structure with a grain size of less than 10 microns was formed in the alloy.

For the technological implementation of torsion with tension, a “running neck” method was proposed [20], the diagram of which is shown in Fig. 7. According to this method, in the heated part of the original rod, an artificial neck is made with the help of rollers, with a diameter 20–25% less than the original diameter of the rod. In it, the material was simultaneously subjected to plastic torsion and tension by means of end grips. After the end of the grain refinement stage in the neck, the roller is returned to its original position, and at the same time the tensile force is reversed to the compression force.

In this case, the divergence of the rollers is synchronized in a way that the surface of the workpiece is rolled until it reaches its original diameter to eliminate macro-irregularities. Next, the carriage with rollers and a local induction heater is moved to a new adjacent position and the above steps are repeated again. Thus, by sequentially moving the deformation zone in the neck, a multi-meter rod with a large-diameter UFG structure is obtained. To increase durability, the temperature of the rolls is maintained 50–100 degrees below the heating temperature of the workpiece.

5.2. Torsion under pressure

For this SPD method, an isothermal stamp for upsetting with torsion was proposed [19]; see Fig. 8 where 1 and 2 are

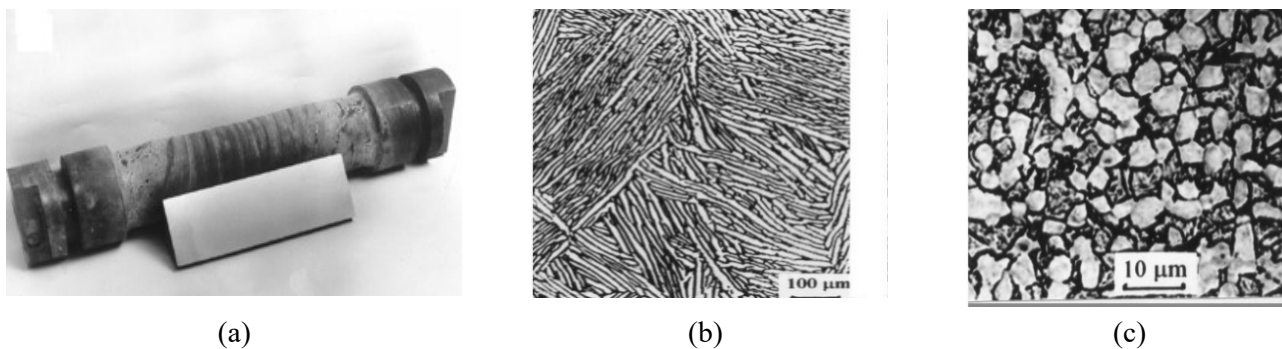


Fig. 6. A sample of two-phase heat-resistant titanium alloy VT9 and its macrotemplate: (a) after tension with torsion; (b) the initial lamellar structure of the sample; (c) homogeneous ultra-fine-grained structure in the zone of localization of combined deformation.

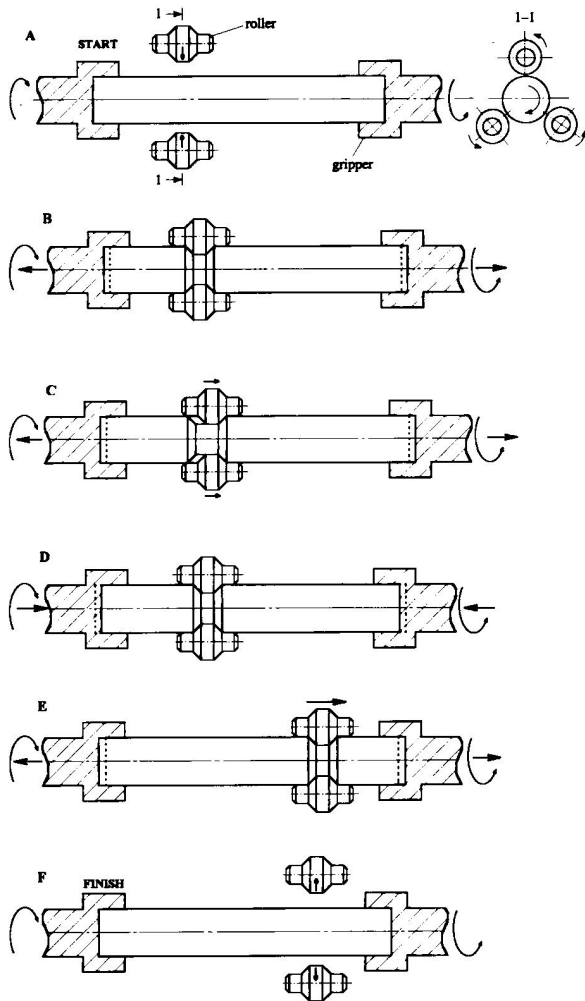


Fig. 7. Scheme for manufacturing rods with UFG structure using the “running torsion neck” method

the upper and lower die plates, 3 is disk, 4 is upper striker, 5 is lower striker, 6 is thermal insulation, 7 is induction heater, 8 is engraving of the lower striker, 9 is engraving of the upper striker, 10, 11 are bearings. 12, 13 is worm gear, 14, 15 are grooves on the die engravings for transmitting torque and using lubricant in the radial direction.

The work principle of the stamp is as follows. A heated and lubricated workpiece with the original coarse-grained structure (hot-deformed, powdered or cast) is installed on the lower striker of a preheated die. The upper striker is lowered and inserted into the workpiece to the extent of the profile of radially directed grooves on the surface of the strikers. The grooves are designed in such a way that in the radial direction they reduce the coefficient of friction due to the use of lubricant, and in the circumferential direction they create a vertical step that ensures the transmission of torque to the workpiece without sliding. The radial component f_r of the friction force on the vertical steps and horizontal elements of the strikers is a reactive force that prevents an increase in the end surface area of the workpiece. Ideally, it should be reduced to zero due to

the optimal geometric shape of the grooves and effective lubrication.

After additional heating of the workpiece to the deformation temperature, which compensates for its cooling when transferred from the electric furnace to the die, the workpiece is upset with simultaneous torsion in the temperature-speed regime of superplastic deformation. The deformation operation is completed when the specified thickness of the workpiece is reached and a stationary value of the torsion moment of the lower striker is established. This mode arises as a result of the formation of a UFG structure, as a result of which a constant minimum value of the flow stress of the workpiece material is achieved. Then reverse torsion of the lower striker is performed to separate the disk from the surface of the strikers. Next, the upper striker is raised, and the disk with the UFG structure is removed from the die area by a manipulator.

6. DISCUSSION OF RESULTS

Non-monotonic deformation is essential in the preparation of UFG structure, both in the case of deformation of coarse-grained material in the regime of superplastic deformation and in the case of SPD. Such deformation provides a periodic change in the orientation of the strain tensor, for example, during all-round forging or multi-transition ECAP. It is more technologically advanced to carry out such a rotation continuously by torsion of the workpiece during its shear deformation. While insignificantly affecting the shape change of the sample, the rotational component leads to a refinement of the microstructure. In the case of deformation in the regime of superplastic deformation of a coarse-grained material, plastic torsion creates many recrystallization centers—sections of boundaries with large curvature, the migration of which leads to the formation of small grains. In this case, a small strain rate kinetically corresponds to the kinetics of mass transfer of alloying elements that ensure the formation of a stable two-phase UFG structure under deformation conditions. Such structures in heat-resistant nickel alloys are microduplex and globular microstructures in titanium heat-resistant alloys [1,13].

In the case of SPD, non-monotonic torsional deformation leads to the formation and intersection of boundaries of deformation origin and the formation of a fine network of grain boundaries. From the viewpoint of physical mesomechanics, such boundaries are those of disclination origin. Their interaction with lattice dislocations ensures the growth of their misorientations to high-angle ones, which leads to the formation of a submicro- and nanometric structure.

The use of isothermal devices for realization of compression with torsion or tension with torsion is advisable

from a practical point of view. All industrial metallurgical semi-finished products of large sizes, including structural heat-resistant alloys, as well as magnesium alloys, are initially produced in the form of castings and coarse-grained forgings, extrusions and rolled products. Direct milling of such materials by SPD methods is difficult, because it would be necessary to refine the grains in a coarse-grained structure by $10^7 \div 10^8$ times. Under isothermal conditions of deformation in the regime of superplastic deformation, small strain rates provide kinetically coordinated rates of hardening and softening necessary for dynamic recrystallization in coarse-grained materials and necessary for phase transformations. Therefore, it is advisable, in the mode of superplastic deformation of heterophase magnesium alloys, first, to form a microcrystalline structure with a uniform distribution of chemical, phase and grain structure. Then, at the second phase of the operation, after temperature reduction to the conditions of warm deformation, continue grain refinement to the submicro- and even nanometric level of the structure, where it will be necessary to reduce the grain size only by $10^2 \div 10^3$ times.

7. CONCLUSION

Based on the analysis of mechanics and physical mesomechanics under large deformation of coarse-grained materials in the temperature-speed regime of superplastic deformation and under SPD conditions, methods of combined torsional deformation with axial deformation-tension or compression are proposed, which make it possible to obtain UFG rods and disks of large diameters with micrometric, submicrometric and nanometric grain sizes.

REFERENCES

- [1] O.A. Kaibyshev, F.Z. Utyashev, *Superplasticity: Microstructural Refinement and Superplastic Roll Forming*, Futurepast, Arlington, VA, USA, 2005, 386 p.
- [2] R.Z. Valiev, A.P. Zhilyaev, T.G. Langdon, *Bulk Nanostructured Materials: Fundamentals and Applications*, John Wiley & Sons, Inc., 2013.
- [3] O.A. Kaibyshev, *Plasticity and superplasticity of metals*, Metallurgiya, Moscow, 1975 (in Russian).
- [4] I.I. Novikov., V.K. Portnoy, *Superplasticity of alloys with ultrafine grains*, Metallurgiya, Moscow, 1981.
- [5] R.Z. Valiev, R.K. Islamgaliev, I.V. Alexandrov, *Bulk nanostructured materials from severe plastic deformation*, *Progress in Materials Science*, 2000, vol. 45, no. 2, pp. 103–189.
- [6] R.Z. Valiev, I.V. Aleksandrov, *Bulk nanostructured metallic materials: preparation, structure and properties*, Akademkniga, Moscow, 2007 (in Russian).
- [7] L.I. Sedov, *Continuum Mechanics, Volume 1*, Nauka, Moscow, 1970 (in Russian).
- [8] F.Z. Utyashev, R.Z. Valiev, G.I. Raab, A.K. Galimov, *Strain Accumulated during Equal-Channel Angular Pressing and Its Components*, *Russian Metallurgy (Metally)*, 2019, vol. 2019, no. 4, pp. 281–289.
- [9] F.Z. Utyashev, Y.E. Beygelzimer, R.Z. Valiev, *Large and Severe Plastic Deformation of Metals: Similarities and Differences in Flow Mechanics and Structure Formation*, *Advanced Engineering Materials*, 2021, vol. 23, no. 7, art. no. 2100110.
- [10] V.V. Rybin, *Large plastic deformations and fracture of metals*, Metallurgiya, Moscow, 1986 (in Russian).
- [11] A.E. Romanov, A.L. Kolesnikova, *Application of disclination concept to solid structures*, *Progress in Materials Science*, 2009, vol. 54, no. 6, pp. 740–769.
- [12] A.P. Zhilyaev, A.I. Pshenichnyuk, F.Z. Utyashev, G.I. Raab, *Superplasticity and Grain Boundaries in Ultrafine-Grained Materials, Second Edition*, Woodhead Publishing, Duxford, UK, 2020.
- [13] O.A. Kaibyshev, F.Z. Utyashev, *Superplasticity, structure refinement and processing of hard-to-deform alloys*, Nauka, Moscow, 2002 (in Russian).
- [14] O.M. Smirnov, A.N. Ershov, V. Kropotov, *Effect of combined loading on stamping parameters of flat disks in state of superplasticity*, *Kuznechno-Shtampovochnoe Proizvodstvo*, 1997, no. 1, pp. 7–9 (in Russian).
- [15] R.L. Athey, J.B. Moore, *Progress Report on the Gatorising™ Forging Process*, SAE Technical Paper 751047, National Aerospace Engineering and Manufacturing Meeting, Los Angeles, 1975.
- [16] R. Athey, J. Moore, *Processing for integral gas turbine disc/blade component*, US Patent No. US3741821A, 1973.
- [17] Ch. Sims, V. Hagel, *Heat-resistant alloys*, Metallurgiya, Moscow, 1976 (in Russian).
- [18] K.A. Padmanabhan, R.A. Vasin., F.U. Enikeev, *Superplastic flow: phenomenology and mechanics*, Springer-Verlag, Berlin, Heidelberg, Germany, 2001, 363 p.
- [19] R.Yu. Sukhorukov, N.F. Koshchavtsev, F.Z. Utyashev, V.A. Valitov, A.R. Ibragimov, *Form for hot deformation of gas turbine engine disc*, Russian Patent No. RU216591U1, 2022.
- [20] F.Z. Utyashev, O.A. Kaibyshev, O.R. Valiakhmetov, *Method for working blanks of metals and alloys*, Russian Patent No. RU2159162C2, 1998.
- [21] V.L. Kolmogorov, *Mechanics of metal forming*, Metallurgiya, Moscow, 1986 (in Russian).
- [22] J. Friedel, *Dislocations*, Mir, Moscow, 1967 (in Russian).
- [23] O.A. Kaibyshev, G.A. Salishchev, R.M. Galeev, R.Ya. Lutfullin, O.R. Valiakhmetov, *Method of treatment of titanium alloys*, Russian Patent No. RU2134308C1, 1996.
- [24] D.A. Hughes, N. Hansen, *Microstructure and strength of nickel at large strains*, *Acta Materialia*, 2000, vol. 48, no. 11, pp. 2985–3004.
- [25] V.V. Rybin, *Patterns of formation of mesostructures during developed plastic deformation*, *Voprosy Materialovedeniya*, 2002, no. 1(29), pp. 11–33 (in Russian).
- [26] J. Martin, R. Doherty, *Stability of the microstructure of metal systems*, Atomizdat, Moscow, 1978 (in Russian).
- [27] I.A. Ditenberg, A.N. Tyumentsev, A.V. Korzikov, E.A. Korznikova, *Evolution of the microstructure of nickel during deformation by torsion under pressure*, *Physical Mesomechanics*, 2012, vol. 15, no. 5, pp. 59–68 (in Russian).
- [28] A.N. Tyumentsev, I.A. Ditenberg, A.D. Karataev, K.D. Denisov, *Evolution of crystal lattice curvature in metallic*

- materials at meso and nanostructural levels of plastic deformation, *Physical Mesomechanics*, 2013, vol. 16, no. 3, pp. 61–77 (in Russian).
- [29] F.Z. Utyashev, *Modern methods of intense plastic deformation: textbook*, UGATU, Ufa, 2008 (in Russian).
- [30] F.Z. Utyashev, G.I. Raab, Deformation methods for the production and processing of ultrafine-grained and nanostructured materials, Ufa, Gilem, NIK Bashk. Enycl., 2013.
- [31] V.M. Segal, V.I. Reznikov, V.I. Kopylov, D.A. Pavlik, V.F. Malyshev, *Processes of plastic structure formation of metals*, Navuka i tekhnika, Minsk, 1994.
- [32] M.A. Shtremel, *Strength of Alloys, Part 1: Lattice Defects: Textbook for universities in the specialties "Physics of Metals", "Metal Science and Heat Treatment of Metals"*, MISIS Publishing House, Moscow, 1999 (in Russian).

УДК 621.77.04+621.73.073

Рациональные методы пластической деформации, обеспечивающие формирование ультрамелкозернистой структуры в крупнозернистых изделиях

Ф.З. Утяшев, А.В. Боткин, Е.П. Волкова, Р.З. Валиев

Уфимский университет науки и технологии, Уфа, 450076, Россия

Аннотация. На основе особенностей механики пластической деформации и физической мезомеханики рассмотрены процессы и предложены технологические схемы их реализации, обеспечивающие формирование ультрамелкозернистой структуры в осесимметричных изделиях больших размеров. В качестве методов подготовки такой структуры взята деформация крупнозернистых материалов в температурно-скоростных условиях сверхпластической деформации и методы интенсивной пластической деформации. Все эти деформации являются большими, их осуществляют с невысокими гидропрессовыми скоростями, но при разных температурах: в режиме сверхпластичности при горячей, а в режиме интенсивной пластической деформации при теплой или холодной температуре деформации. Первый режим позволяет измельчать зерна до микрокристаллических размеров 1–10 мкм, и такой материал приобретает возможность уже деформироваться в состоянии сверхпластичности, т.е. при растяжении с небольшим сопротивлением деформации и с большим удлинением. Второй режим, т.е. интенсивная пластическая деформация, измельчает зерна до субмикро- ($1 \div 0.1$ мкм) и наноразмеров менее 0.1 мкм, придавая, тем самым, металлическим материалам рекордную конструкционную прочность, а также возможность использовать обработку в расширенных температурно-скоростных условиях сверхпластической деформации в сравнении с микрокристаллической структурой.

Ключевые слова: ультрамелкозернистая структура; сверхпластическая деформация; интенсивная пластическая деформация; сдвиговая и ротационная деформации; кручение с осадкой или с растяжением